

Cover Page



Universiteit Leiden



The handle <http://hdl.handle.net/1887/30206> holds various files of this Leiden University dissertation.

Author: Rabe, Martin

Title: Coiled-coils on lipid membranes : a new perspective on membrane fusion

Issue Date: 2014-12-18

Chapter VI

**Can one methylene group make a difference?
Influence of lysine snorkeling
on the activity
of fusogenic coiled-coil peptides**

ABSTRACT

The state of the fusogenic coiled coil forming peptides E and K when tethered to lipid membranes was studied in detail in the recent chapters and it was hypothesized that the interaction of K with the membrane plays a significant role in the mechanism of lipopeptide-mediated membrane fusion. In this chapter a proof of this hypothesis is attempted. The membrane interaction of amphipathic helices of the class A type, such as peptide K, is thought to be enhanced by snorkeling of lysine side chains, i.e. their bending towards a more polar environment. It is shown here, that inhibition of this mechanism in K-variants with shortened lysine side chains significantly reduces the membrane affinity of the peptide and its binding affinity to peptide E. However, when tethering these K-homologues in form of lipopeptides to vesicles, membrane fusion with CPE was not inhibited as anticipated due to unexpected changes of the peptides' lipid affinity at the bilayer. Nevertheless, these results allow for important conclusions about the molecular details of the K-membrane and E/K interactions.

INTRODUCTION

The understanding of the mechanism of vesicle fusion mediated by coiled-coil forming lipidated peptides such as LPE, LPK, CPE, and CPK studied in the last chapters and several vesicle fusion studies,¹⁻⁶ is thought to allow the specific enhancement of such systems. The initial inspiration for these synthetic membrane-fusion model systems was derived from natural SNARE (soluble NSF attachment protein receptor) proteins. These play a central role in the complex protein machinery that drives specific intracellular membrane fusion, for instance in neuronal release of neurotransmitters.⁷⁻⁹ The SNARE proteins are known to dock, fusing vesicles to the target membrane by the formation of a 4-helix coiled-coil bundle. Although the molecular players were identified in recent years, the precise sequence of molecular events in neuronal vesicle fusion remains a highly debated topic.⁸⁻¹² Despite the differences, a common feature in the various models is that docking of the vesicles to the target membrane is necessary but does not provide sufficient energy to enable full bilayer merging. Instead, mechanisms are under discussion that involve stress generation or destabilization in the prefusion membrane, with this stress or destabilization being released after fusion. This can for instance be a pulling force that arises from the zippering of the spacer region of the SNARE complex into a rigid coiled-coil from the prefusion trans- to the postfusion cis- complex,^{8,9} or a specific Ca^{2+} -dependent wedge like incorporation of synaptotagmin into one leaflet of the bilayer.¹⁰⁻¹³

In the synthetic fusogenic lipopeptide systems the coiled-coil forming peptides E and K are tethered to the membrane anchor via a polyethylene glycol spacer. A transfer of a pulling force into the bilayer by such a flexible moiety appears questionable. However, in *Chapters III-IV* evidence was presented that K incorporates into lipid mono- and bilayers with its helical axis parallel to the membrane plane due to its amphipathic character. The amphipathic helix of class A that was proposed as the membrane interacting form might therefore form the necessary peptide wedge that creates sufficient membrane curvature to promote the bilayer merging. A possible approach to prove such a mechanism is the targeted inhibition of the peptide membrane interaction which is anticipated to drastically reduce fusion efficiency. This inhibition could be achieved by varying the lipid composition, aiming for a non-binding composition. The challenge in this approach will be to ensure that the physical properties of the membrane are not changed too drastically allowing fusogenicity to be retained. Unpublished results from Martelli et. al. imply the feasibility of this approach.¹⁴

An alternative strategy that will be followed in this chapter is to use a negative redesign approach, i.e. to inhibit the peptide membrane interaction by varying the peptide primary structure.¹⁵ The challenge with this approach will be to retain

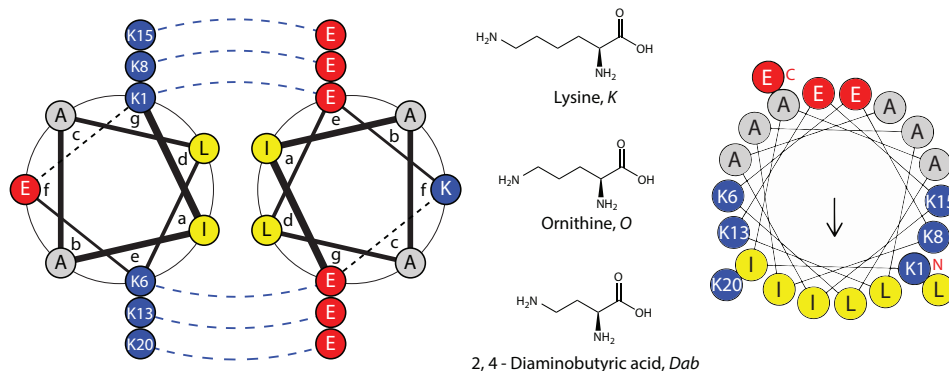
the coiled-coil binding propensity and specificity of K as these properties are anticipated to have an influence on vesicle docking and therefore fusion efficiency.^{3,6} A disruption of the amphipathic helix or a change of the overall charge of K should, in principle, inhibit the helical membrane incorporation, although such a strong change will also significantly change the binding properties. Thus, the sequence variation should be relatively subtle.

A characteristic property of the helical wheel of K is its regularity, which is a consequence of its uniform primary structure. The positions of the heptad repeat, (*a...g*) which is the typical repeating sequence pattern in coiled-coils, are uniformly filled with the same amino acids (Chart 1).^{16,17} This regular primary structure also leads to a very uniform distribution in the standard α -helix with 3.6 residues per turn. This distinct arrangement with the positively charged residues orthogonal to the hydrophobic moment and the negatively charged ones central on the polar face was categorized as a class A amphipathic helix, which is common in apolipoproteins and interacts with lipid interfaces.^{18,19}

It was proposed that the relatively long lysine side chains, often found in the orthogonal position of the class A helices, bend towards the polar face which increases the surface of the hydrophobic face and brings the charged tips into a more favorable polar environment (Figure 1).¹⁹⁻²⁵ This process, called snorkeling, creates a wedge shaped cross section and allows the helix to penetrate more deeply into the hydrophobic interior of the lipid bilayer and thus enhances its membrane affinity. One way to limit the effectiveness of snorkeling is to substitute the lysines with ornithine or 2, 4- diaminobutyric acid, i.e. amino acids whose side chains are, respectively, one or two methylene units shorter than lysine but contain the same terminal amino functionality (Chart 1).²¹ However such a relatively subtle change still can have a substantial influence on the binding properties of a coiled coil complex as electrostatic *g/e'* interactions, i.e. between the *g* position of one helix and the *e* position of the subsequent heptad of the other helix, are affected and are known to contribute to the binding energy (Chart 1).^{15,26-29}

In this chapter, the design of K homologues with shortened lysine side chains is reported. The coiled coil binding properties in homo- and hetero complexes with E are studied in detail. Furthermore, the membrane interactions of the K-homologues are probed, which substantiates the principle feasibility of the chosen negative design approach and the influence of snorkeling on the membrane interaction of K. From this initial set of K-homologues, the most promising candidates with regard to little membrane and reasonable E binding were chosen and CPK lipopeptide homologues based on these K homologues were synthesized. These CPK homologues were then tested for their ability to induce membrane fusion.

Chart 1. Helical wheel projection of the E/K coiled coil complex, with potential ionic interactions marked as broken lines; chemical structures of lysine, ornithine, and 2, 4 – diaminobutyric acid; helical wheel projection of K as a monomeric α -helix, the arrow indicates the direction of the hydrophobic moment. Images created by means of ‘Draw-Coil 1.0’ and ‘HeliQuest 2’.^{16,17}



RESULTS AND DISCUSSION

PEPTIDE DESIGN

Peptide K was redesigned using shorter lysine analogues in order to reduce the snorkeling ability of the peptides whilst leaving the overall amphipathic helix and the charge distribution intact as these factors are important for maintaining coiled coil binding and specificity. Ornithine (O) with one methylene unit shorter, and 2, 4 – diaminobutyric acid (Dab) with two methylene units shorter, were used to substitute all lysine residues in the *e* and *g* positions of the heptads which gave the peptides O_6 and Dab_6 (Chart 1 and Table 1).

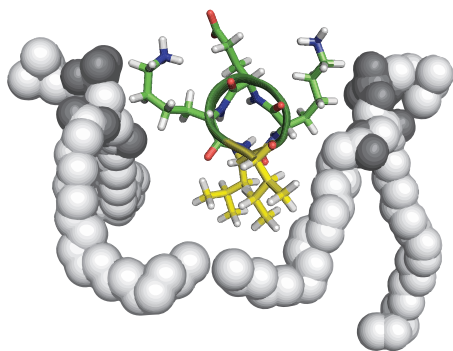


Figure 1. Illustration of the snorkeling mechanism of the *LKEKI* sequence of peptide K. View from the C-terminus. Long chained positively charged lysine residues bend towards the polar face. Carbons of hydrophobic *I* and *L* residues are depicted in yellow, carbons of polar residues *K* or *E* are green. Nitrogen, oxygen, and hydrogen atoms are blue, red and white, respectively.

It was found that these substitutions strongly influenced the coiled-coil binding strength (see below). Thus, to obtain a variant of K that more closely resembles the binding properties of the original E/K pair, further derivatives were synthesized with partial substitutions of the lysines. The peptides K_3O_3 and O_3K_3 had all *e*, or all *g*, positions substituted with ornithine; and the peptide $K_2O_2K_2$ had the two middle lysines, K8 and K13, substituted with ornithine residues (Table 1). All peptides were synthesized using solid phase peptide synthesis.

Table 1. Overview of the studied peptides.

Short name	Substitution ^a	Sequence ^a
E		Ac-(EIAALEK) ₃ -NH ₂
K		Ac-(KIAALKE) ₃ -NH ₂
Dab ₆	K1, K6, K8, K13, K15, K20 = Dab	Ac-(DabIAALDabE) ₃ -NH ₂
O ₆	K1, K6, K8, K13, K15, K20 = O	Ac-(OIAALOE) ₃ -NH ₂
O ₃ K ₃	K1, K8, K15 = O	Ac-(OIAALKE) ₃ -NH ₂
K ₃ O ₃	K6, K13, K20 = O	Ac-(KIAALOE) ₃ -NH ₂
K ₂ O ₂ K ₂	K8, K13 = O	Ac-KIAALKE OIAALOE KIAALKE-NH ₂

^aOrnithine residues are denoted by O; 2, 4 – diaminobutyric acid residues are denoted by Dab

COILED-COIL BINDING

Circular dichroism (CD) spectroscopy was used to determine the binding properties of the peptides. First, the tendency of all peptides to form homomeric coiled-coil complexes was tested by means of temperature dependent circular dichroism (CD) spectroscopy. The mean residue ellipticity at 222 nm ($[\theta]_{222nm}$) is a convenient measure for the helical content and melting curves based on this measure yield valuable insight as to the thermodynamics and molecularity of the complex folding (Chapter II).³⁰⁻³³ The $[\theta]_{222nm}$ temperature curves of E and K showed increasing ellipticities reaching a plateau, which indicates a cooperative unfolding of the helical peptides. Similar observations were found for the tryptophan labeled variants E_{GW} and K_{GW} of these peptides in Chapter II and can be interpreted as the unfolding of the homomeric coiled coils E/E and K/K (see below). In contrast the $[\theta]_{222nm}$ curves of the peptides containing Orn and Dab displayed no temperature dependent unfolding behavior and their spectra showed the characteristics of unstructured peptides (Figure A1 and Figure A2). Thus, the homo-coil formation is strongly inhibited by the shortened side chains.

The comparison of the behavior of E with O₆ indicates that, despite Orn and Glu having equal side-chain lengths, the carboxylate group of the glutamic acid residues are preferred for homo coil formation over the ammonium groups of ornithine. Both the homo coil inhibition with shorter chain lengths and the preference of the carboxylate in the homo coil were reported by Ryan and Kennan, who studied the chain length influence in the *e* and *g* positions of an acidic and basic coiled-coil pair acid-p1/base-p1.²⁷ Thus, they appear to be general effects and illustrate the importance of electrostatic interactions between residues in the *g* and *e'* positions. A possible explanation for these effects might be a mechanism similar to the snorkeling of lysine side chains in the amphipathic A helix. In the relatively unstable E/E and K/K homocoils the side chains in the *e* and *g* positions might reduce the

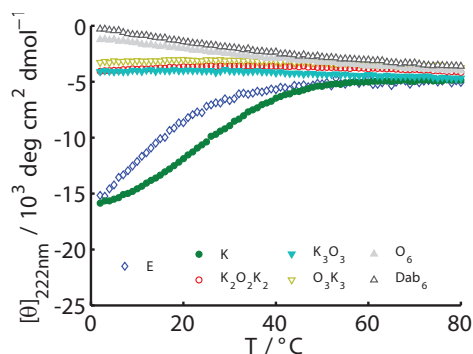


Figure 2. Temperature dependency of mean residue ellipticity at 222 nm of E, K, and K- homologues. Experimental conditions: [peptide] = 100 μ M, buffer: PBS, pH 7.4.

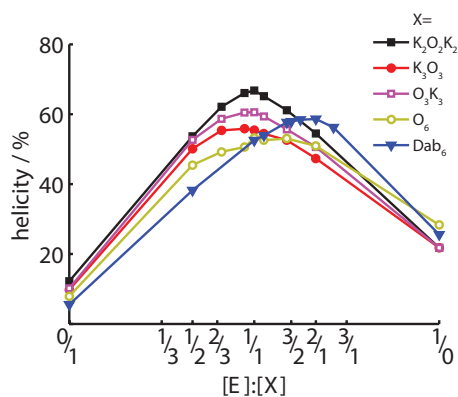


Figure 3. Job plot of the coiled coil complexes composed of E and K homologues (X) at constant total monomer concentrations $[E] + [X] = 200 \mu\text{M}$.

The peptides K_3O_3 , O_3K_3 and $K_2O_2K_2$ showed maximum helical content at $[E]:[X]$ of 1 : 1, which implies that they form a complex with equal numbers of chains of both binding partners, i.e. their stoichiometric ratio ($\nu_E : \nu_X$) is also 1 : 1. For Dab_6 the maximum helical content is found at $[E]:[Dab_6] = 2 : 1$, implying this stoichiometric ratio for the coiled-coil complex. The Job plot of O_6 is broader, compared to the others, which might either be caused by several complexes of different stoichiometric ratios or a relatively low binding constant.³⁷

Temperature and concentration dependent CD unfolding curves of the peptide complexes were measured, to determine the thermodynamics of un-folding and the molecularity (n) of the unfolding process (Figure A3 - Figure A10). All studied complexes including the homocoils of E/E and K/K showed shifts of the unfolding curves to higher temperatures with increasing total peptide concentration, implying that all

repulsive ionic interactions by bending away from the binding partner. The reduction of this ability might therefore explain the inhibited homocoiling in the side-chain shortened K-homologues.

To test if the K derivatives form coiled-coil complexes with E, Jobs method^{34,35} was applied, i.e. $[\theta]_{222nm}$ was used to determine the helicity as a function of the molar ratio of E to its binding partner X ($[E]:[X]$), while leaving the total peptide concentration ($[E] + [X]$) constant (Figure 3). When E was mixed with the different binding partners, the CD spectra showed the typical shape of helical peptides with minima at 208 nm and 222 nm (Figure A1 and Figure A2). Based on $[\theta]_{222nm}$ all K-variants showed an increased helical content when mixed with E, compared to the peptides alone at $[E]:[X] = 0 / 1$, or 1 / 0 respectively. This shows that E interacts with all the binding partners and forms heteromeric coiled-coil complexes. For the complex E/K, the stoichiometric ratio is known to be 1 : 1.³⁶

observed unfoldings involve more than a single peptide chain (*Chapter II*).^{38,39} The data were fitted to thermodynamic unfolding models of different molecularities. The unfolding curves of all peptide complexes except E/Dab₆ were best fitted by models with $n = 2$, based on the minimum root mean square error of the fits (RMSE, Figure 4). This means that these peptides form predominantly dimers in solution. The only exception, E/Dab₆, gave good fitting models with molecularities of 3 and 4. Taking into account the result of Jobs method, which implied a stoichiometric ratio in the complex of 2 : 1, this indicates that the coiled-coil complex is trimeric with two chains of E and one chain of Dab₆.

The best fitting models also yielded the thermodynamics of the unfolding with the parameters ΔH° , T° and ΔCP , which allows the prediction of the complex stability at every temperature (Table A1). These parameters were used to calculate the free enthalpy of unfolding per monomer chain as well as the folding constant at 25 °C ($\Delta G_{25} / n$ and K_{F25}), which allows for a comparison of the stability of the different coiled complexes (Figure 5 and Table 2). The original sequence of E/K was found to be the most stable of the studied complexes with the highest ΔG_{25} and K_{F25} . Shortening of the side chains in the *e* and *g* positions led, in every case, to a reduction of the free enthalpy per chain. The E/O₆ dimer was found to be the least stable of the heterodimers. Compared to that, the unfolding free enthalpy of E/Dab₆ is increased, showing that the formation of the trimer compensates for the loss of unfolding energy upon shortening of the side chains.

The peptide pairs with mixed ornithine and lysine side chains E/O₃K₃, E/K₃O₃, and E/K₂O₂K₂ showed intermediate stabilities and folding constants in the same order of magnitude (Table 2). It appears that the position of substitution in the helix has an influence on the unfolding free enthalpy, although definitive conclusions are difficult due to the low significance of the differences. The unfolding free enthalpy of the homo coils K/K and E/E was found to be the smallest, which is due to the repulsive interactions of identically charged residues in the *e* and *g* position in these complexes.

The general trend of the decreasing dimeric hetero coiled-coil stability with the decreasing chain length of charged residues in the *e* and *g* positions is in line with the results reported by Ryan and Kennan for the homologues of acid-p1/base-p1.²⁷ In their study the side chain shortened variants were forced into a dimeric state by single buried asparagine residues in the *a* position of the heptad and the shortening of the basic side chains up to 2, 3-diaminopropionic acid resulted in a strong destabilization of these complexes. A comparable effect for the *b* and *c* positions in tetrameric complexes was also reported by Vu et. al.²⁶ The reason for the effect in the dimers appears to be the ability of the longer side chains in the *e* position to get closer to the oppositely charged residue in the *g'* position of the neighboring peptide,

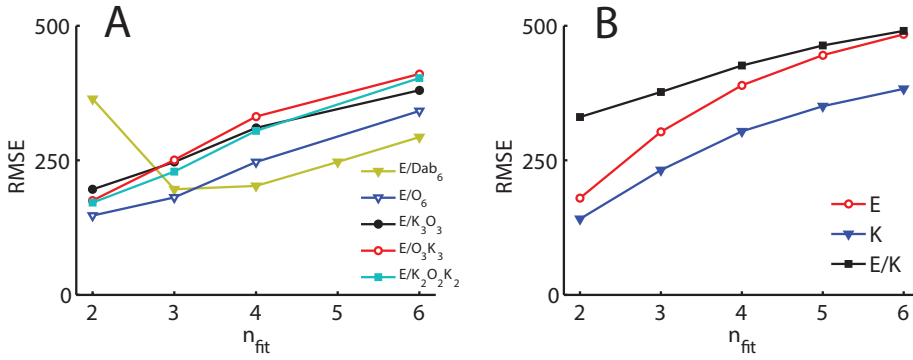


Figure 4. Root mean square errors of best fits with different models ($n_{fit} = 2 \dots 6$) for (A) the coiled coils of E with the K homologues E/X; (B) E, K and E/K. Data was fitted using *FitDis!*. For data, best fitting models, and fit parameters see appendix.

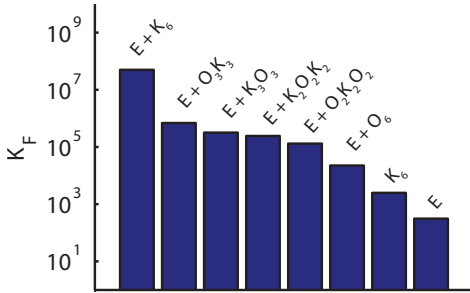


Figure 5. Free enthalpy of peptide folding at 25 °C per chain monomer of all studied peptide complexes.

Table 2. Folding constants of studied coiled coil complexes at 25 °C

Coiled coil	K_{F25}
E/K	$3.7 \cdot 10^6 \text{ M}^{-1}$
E/KDab	$1.7 \cdot 10^9 \text{ M}^{-2}$
E/O3K3	$6.9 \cdot 10^5 \text{ M}^{-1}$
E/K3O3	$3.2 \cdot 10^5 \text{ M}^{-1}$
E/K2O2K2	$2.4 \cdot 10^5 \text{ M}^{-1}$
E/Korn	$2.3 \cdot 10^4 \text{ M}^{-1}$
K/K	$2.5 \cdot 10^3 \text{ M}^{-1}$
E/E	$3.1 \cdot 10^2 \text{ M}^{-1}$

which increases attractive ionic interactions and stabilizes the dimeric state. In a molecular dynamics study, Pendley et al. predicted a drastically reduced coiled-coil binding propensity of E/O₆, due to the reduction of this stabilizing effect,²⁸ which is in line with the results reported here. This stabilizing effect was even stronger reduced for E/Dab₆, destabilizing the potential dimer so far that the trimer was formed. The trimeric state is thought to be a relatively stable oligomeric default state for coiled-coils, that is adopted in the absence of strong determinants of oligomeric state.¹⁵

The aim of the present study is to find a homologue for peptide K with suppressed membrane interactions while retaining the oligomeric state and the binding strength as much as possible. Considering these criteria, the variants with mixed lysine and ornithine residues in *e* and *g* positions appeared to be the best candidates for the further studies.

PEPTIDE MEMBRANE INTERACTIONS

To probe if the peptides interact with membranes as the original K, the temperature dependency of $[\theta]_{222nm}$ was measured for the peptides mixed with vesicles of the composition DOPE : DOPE : Cholesterol 2 : 1 : 1 (Figure 6). Strikingly, mixing with vesicles had no significant influence on any of the K homologues, while $[\theta]_{222nm}$ of K mixed with vesicles showed the typical decrease due to its increased helicity over the whole temperature range as known from *Chapter V*.

Thus, the interactions of the K homologues with the membrane are drastically reduced as was intended by the negative peptide design. The chain length of the positively charged side chains placed orthogonally to the amphiphatic moment in the A-helix has a strong influence on membrane incorporation, which can be explained by the snorkeling of these chains. The longer lysine side chains are thought to allow a deeper penetration of the amphiphatic A-helix into the lipid bilayer as they can bend further towards the hydrophilic face of the helix.^{19,21,25} A deeper possible penetration depth increases the peptides' lipid affinity, due to an increased hydrophobic interaction.

Mishra et. al. showed reduced lipid affinity for a homologue of the model peptide 18A where all 4 lysine residues were substituted by 2, 4-diaminobutyric acid.²¹ Interestingly, it is shown here that shortening of only the two central lysine side chains in a helix with 5.8 turns as in $K_2O_2K_2$ significantly decreases the lipid affinity of the helix. Also, shortening on one side of the helix as in K_3O_3 and O_3K_3 gives this effect which shows that the cooperative snorkeling of several lysine side chains is responsible for the relatively high lipid affinity of K.

LIPOPEPTIDE MEDIATED VESICLE FUSION

As all the tested peptides showed a reduced lipid affinity compared to K with no measurable lipid induced helix formation (Figure 6), they all appeared suitable for generating lipopeptide variants of CPK with reduced lipid interaction. Taking the binding properties into account, O_3K_3 and $K_2O_2K_2$ were chosen for further experiments as they were found to form dimeric hetero coils with E and most closely resemble the binding affinity of the original sequence. The lipopeptides CPO_3K_3 , $CPK_2O_2K_2$, CPK, and CPE were synthesized using standard methods (Chart 2).^{2,5}

To study the lipopeptides ability to mediate membrane fusion, two sets of liposomes of the composition DOPE : DOPE : Cholesterol 2 : 1 : 1 in PBS were prepared. One set contained CPE and the other CPK or its homologues $CPK_2O_2K_2$ and CPO_3K_3 , the lipopeptide concentration with respect to the total lipid concentration in all vesicles was 1 mol%. Vesicle fusion can be identified by three hallmarks: aggregation; lipid mixing; and content mixing (Figure 7).^{1-6,40} Aggregation

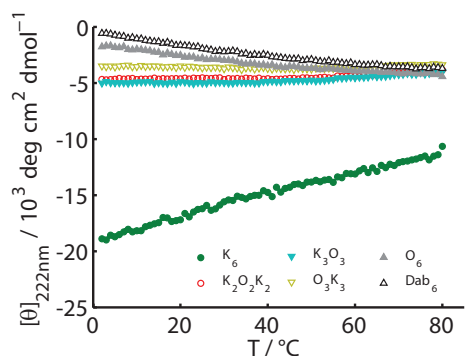
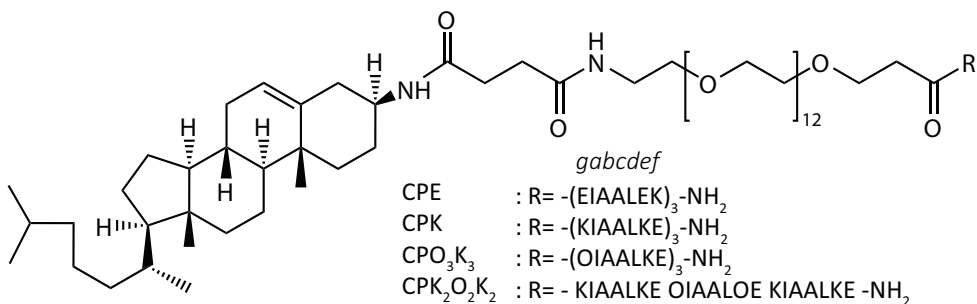


Figure 6. Temperature dependency of mean residue ellipticity at 222 nm of E, K, and K- homologues mixed with DOPE : DOPE : Cholesterol (2 : 1 : 1) vesicles. Experimental conditions [lipid] : [peptide]=25 : 1, [peptide] = 100 μ M.

dyes. Finally, content mixing is measured using the self-quenching fluorescent dye sulforhodamine B, which is encapsulated in CPE containing vesicles.^{4,5} Upon content mixing the dye is diluted, which leads to an increase in fluorescence intensity, here the 100% reference was the fluorescence of vesicles lysed by detergent. The 0% reference value in both content and lipid mixing experiments was the fluorescence of CPE vesicles mixed with vesicles lacking the binding partner.

Contrary to expectations, vesicles labeled with CPO_3K_3 and $\text{CPK}_2\text{O}_2\text{K}_2$ showed all three hallmarks of fusion upon mixing with CPE containing vesicles (Figure 7). The hydrodynamic radii (r_h) increased after mixing of the vesicles and the lipid and content mixing assays showed fluorescence increases comparable to the original CPK. Thus, the anticipated inhibition of fusion could not be observed and vesicle fusion is mediated also by the side chain shortened homologues of CPK.

Chart 2. Chemical structure of lipopeptides CPE, CPK, CPO_3K_3 , and $\text{CPK}_2\text{O}_2\text{K}_2$. Positions of the amino acids in the heptad repeat are denoted with the letters a...g, Ornithine residue are denoted with O



of vesicles can be measured by means of dynamic light scattering. The mixing of lipids within the bilayer is measured by means of lipids fluorescently labeled with lissamine rhodamine B (LR-DOPE) and 7-nitro-2-1,3-benzoxadiazol-4-yl (NBD-DOPE) which are incorporated into the CPE containing liposomes.^{40,41} Mixing of this bilayer with a label-free bilayer results in the reduction of Förster resonance energy transfer (FRET) and consequently gives an increase in the FRET donor fluorescence (DOPE-NBD). The 100% reference is the fluorescence of liposomes containing only half of the

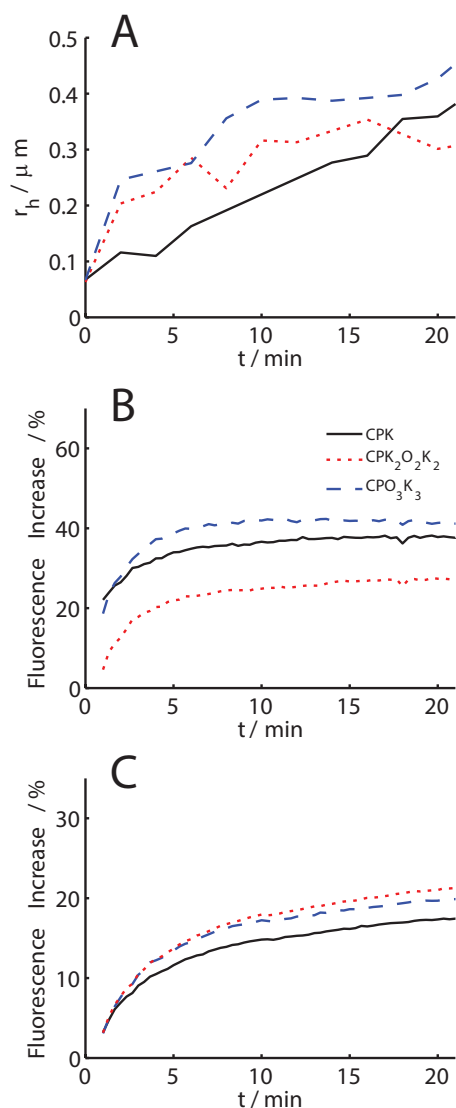


Figure 7. Results of vesicle fusion experiments. Mixing of CPE decorated liposomes with CPK (black line), CPK₂O₂K₂ (red line), or CPO₃K₃ (blue line) resulted in (A) increase of hydrodynamic radius as measured by DLS; (B) lipid mixing, measured by increase of DOPE-NBD fluorescence in FRET experiments; and (C) mixing of vesicle contents, measured by increase in sulforhodamine B fluorescence. In all experiments: lipopeptide concentration 1 mol%; [lipid] = 100 μM ; buffer: PBS pH 7.4 in (A) and (B); TES pH 7.4 in (C).

To reassess whether the interactions of the lipopeptides with the membrane are indeed inhibited as anticipated, $[\theta]_{222\text{nm}}$ of lipopeptide containing vesicles was measured as a function of the temperature (Figure 8). Surprisingly, the membrane tethered CPK₂O₂K₂ and CPO₃K₃ showed a reduced mean residual ellipticity compared to the untethered K₂O₂K₂ and O₃K₃ in a mixture with vesicles. This shows that the helical content is significantly increased. It is unlikely, that this increased helical content is caused by the formation of homomeric coiled coils on the membrane, because in this case $[\theta]_{222\text{nm}}$ would display a typical sigmoidal shape of a cooperative unfolding as was shown for CPE (Chapter V). Instead, the $[\theta]_{222\text{nm}}$ curves overlap largely with the graphs of vesicle tethered CPK and vesicles mixed K (Figure 8), i.e. they show similar slopes and values of helicity. Thus this data indicates, that the CPK homologues CPK₂O₂K₂ and CPO₃K₃ partially fold into α helices and interact with the membrane they are tethered to as was found for membrane tethered K (Chapters III-V).

This means that the interaction of these peptides with the membrane is strengthened due to their tethering to the membrane. The full CD spectra at 25 °C of the untethered peptides K₂O₂K₂ and O₃K₃ showed only very little effect upon mixing with vesicles (Figure 9). The membrane tethered CPK₂O₂K₂ and CPO₃K₃ however, clearly showed spectra with more pronounced minima at 222 nm

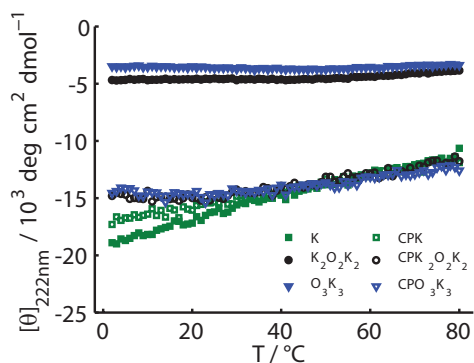


Figure 8. Temperature dependency of mean residue ellipticity at 222 nm of K, $K_2O_2K_2$, and O_3K_3 mixed with vesicles and vesicle tethered CPK, $CPK_2O_2K_2$, and CPO_3K_3 . Experimental conditions [lipid] : [peptide] = 25 : 1, [peptide] = 100 μ M; [lipid] : [CPX] = 100 : 1, [CPX] = 10 μ M, lipid composition DOPE : DOPE : Cholesterol (2 : 1 : 1), in PBS, pH7.4.

and 208 nm, indicative of the formation of helices. A similar increase of the peptide membrane interactions due to membrane tethering was also reported for the lipopeptides LPK in monolayer experiments (*Chapter III*) and LPK_{GW} in tryptophan fluorescence measurements (*Chapter IV*) and appears to be a general property of these systems, although the reasons for this are unclear at this moment. Unfortunately this effect also causes $CPK_2O_2K_2$ and CPO_3K_3 to resemble CPK in their membrane interactions and makes drawing significant conclusions on the effect of these interactions on lipopeptide mediated membrane fusion impossible.

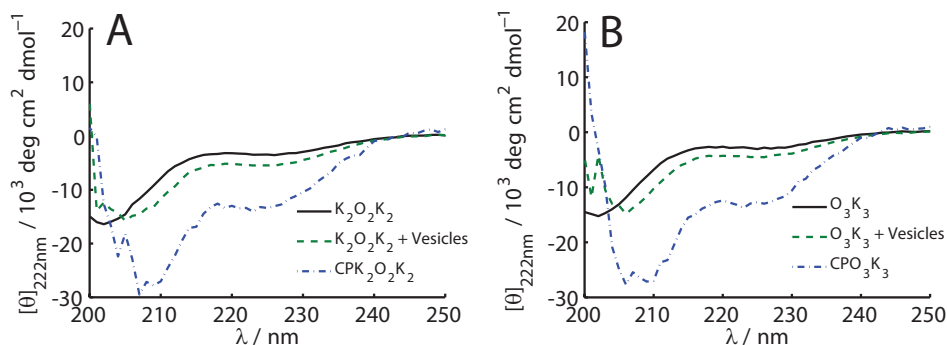


Figure 9. Circular dichroism spectra at 25 °C of (A) $K_2O_2K_2$, $K_2O_2K_2$ mixed with vesicles, and vesicle tethered $CPK_2O_2K_2$; (B) O_3K_3 , O_3K_3 mixed with vesicles, and vesicle tethered CPO_3K_3 . Experimental conditions are the same as in Figure 9.

CONCLUSIONS

The shortening of the lysine side chains in the *e* and *g* positions of the heptad repeat of peptide K had an inhibiting effect on both its coiled-coil formation with E and its lipid affinity. Both properties are determined by similar structural constraints of K and a targeted inhibition of one without influencing the other remains challenging if not impossible.

A substitution of all six lysines by ornithine led to very weak E binding and a substitution with six 2, 4 - diaminobutyric acid further destabilized the dimer and more stable trimers were the predominant species in solution. Partial substitution

yielded stronger binding that more closely resembles the properties of the original K. None of the K-homologues showed a strong α -helical interaction with lipids used in vesicle fusion experiments. This proves that lysine snorkeling makes a substantial contribution to the lipid affinity of K. However when tethered to the lipid membrane in the form of lipopeptides, CPK₂O₂K₂ and CPO₃K₃ resemble CPK in helicity and show an increased membrane interaction. Accordingly, their ability to mediate membrane fusion with CPE labeled vesicles is similar to CPK.

This approach to the study of the influence of the peptide membrane interactions on the lipopeptide mediated fusion by shortening the lysine side chains turned out to be complicated by the multiple effects such a variation causes and has not yet been successful. Furthermore it became apparent that untethered peptides with low lipid affinity can display a different behavior once tethered to the membrane and this was unexpected. In future, this behaviour should be considered when predicting lipopeptide properties on the basis of peptide properties.

EXPERIMENTAL SECTION

MATERIALS

Fmoc-protected amino acids and Sieber Amide resin for peptide synthesis were purchased from Novabiochem. DOPC (1,2-dioleoyl-sn-glycero-3-phosphocholine), DOPE (1,2-dioleoyl-sn-glycero-3-phosphoethanolamine), cholesterol, NBD-DOPE (1,2-dioleoyl-sn-glycero-3-phosphoethanolamine-N-(7-nitro-2-1,3-benzoxadiazol-4-yl) (ammonium salt)), and LR-DOPE (1,2-dioleoyl-sn-glycero-3-phosphoethanolamine-N-(lissamine rhodamine B sulfonyl) (ammonium salt)) were purchased from Avanti Polar Lipids. Solvents, sulforhodamine B, and buffer salts were purchased from Sigma-Aldrich. All water was ultrapure with resistance $\geq 18 \text{ M}\Omega \text{ cm}^{-1}$ and TOC $\leq 2 \text{ ppm}$ produced from a MilliQ Reference A+ purification system. All experiments were carried out in phosphate buffered saline (PBS) of the following composition: 150 mM NaCl, 20 mM PO₄³⁻ in H₂O at pH 7.4.

PEPTIDE SYNTHESIS

The peptides E: Ac-(EIAALEK)₃-NH₂, K: Ac-(KIAALKE)₃-NH₂, were synthesized using standard Fmoc-chemistry on a Biotage Syro I and purified by RP-HPLC to yield a purity > 95% based on HPLC. Identity of the peptides was determined by LC-MS. The lipopeptides were synthesized and purified as described elsewhere.^{2,5} Peptide stock solutions in PBS were prepared at concentrations of ~2 mg/ml, the concentration was based on the mass. Lipopeptide stock solutions were prepared in a CHCl₃:MeOH 3:1 solution and added to the lipids prior to solvent evaporation.

VESICLE PREPARATION.

Lipid stock solutions of the compositions DOPE : DOPE : Cholesterol (2 : 1 : 1) and DOPE : DOPE : Cholesterol : NBD-DOPE : LR-DOPE (49.5 : 24.75 : 24.75 : 0.5 : 0.5) were prepared in CHCl_3 : MeOH 3 : 1. For experiments with lipopeptides, stock solutions were mixed with CPE, CPK, $\text{CPK}_2\text{O}_2\text{K}_2$ or CPO_3K_3 stock solutions in CHCl_3 /MeOH to yield mixtures with 1 mol% lipopeptide content. Lipid films were created by slow evaporation of the solvent from a precise amount of stock solution under a N_2 stream and kept under vacuum overnight. The films were rehydrated with PBS yielding final lipid concentrations of typically 0.1 – 2.5 mM. Large unilamellar vesicles (LUVs) were formed by sonication at 55°C for ~10 min. The size of the vesicles was tested by DLS using a Malvern Zetasizer nano-s and was typically found to be ~100 nm.

CIRCULAR DICHROISM SPECTROSCOPY

CD spectra were measured using a Jasco J815 CD spectrometer equipped with a Jasco PTC 123 peltier temperature controller. Quartz cuvettes with pathlengths l of 1 or 2 mm were used. Spectra were measured from 190 nm to 250 nm with a bandwidth of 1 nm, baseline corrected and the mean residue ellipticity $[\theta]$ was calculated by:

$$[\theta] = \frac{\theta}{l c_M N} \quad (1)$$

where θ is the observed ellipticity, l the pathlength, c_M the molar total peptide concentration and N the number of amino acids per peptide.

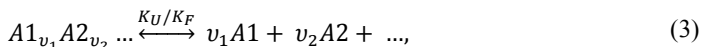
For Job plots at 25 °C the relative peptide ratio of E to its binding partner $[E] : [X]$ was varied between 0 : 10 and 10 : 0 while leaving the total peptide concentration $[E] + [X]$ constant at 200 μM . The relative α - helicity (rh) was calculated from the ellipticity at 222 nm $[\theta]_{222\text{nm}}$ by:^{30,31}

$$rh = \frac{[\theta]_{222\text{nm}}}{-40 \cdot 10^3 \text{ deg cm}^2 \text{ dmol}^{-1} \left(1 - \frac{4.6}{N}\right)} 100\% \quad (2)$$

For probing of peptide-lipid interactions, peptide stock solutions were diluted with buffer to the desired total peptide concentration and eventually mixed with vesicles at $[\text{Lipid}] : [\text{Peptide}] = 25 : 1$ at 100 μM total peptide concentration. Spectra of the lipopeptides tethered to vesicles were measured at $[\text{Lipid}] : [\text{CPX}] = 100 : 1$ in 1 mM total lipid concentration.

For temperature dependent unfolding experiments, peptide stock solutions were diluted with buffer to the desired total peptide concentrations in the range 5 - 200 μM for the hetero coiled-coil complexes and in the range 100 – 1000 μM for

the weaker binding homo coiled-coil complexes of E and K. $[\theta]_{222nm}$ was measured as a function of temperature T at a heating rate of 40 °C / h in the range 2 – 95 °C. Additionally, CD spectra between 190 - 260 nm were collected at $T = 5, 25$ and 80 °C. Spectra taken at 5 °C before and directly after a full heating cycle were found to be fully reproducible. The data was analyzed by means of the thermodynamic formalism described in detail *Chapter II* using the program *FitDis!*. The general equilibrium for the 2 state unfolding of an n -meric folded peptide complex into n monomers with the folding and unfolding constants K_F and K_U is:



where the molecularity n is the sum of the stoichiometric factors v_i ($n = \sum v_i$). The equilibrium constants give access to the free enthalpy of unfolding (ΔG) by:

$$[K_U] = e^{\frac{-\Delta G}{RT}} \quad (4)$$

with the absolute temperature T and the gas constant R . The temperature dependency of ΔG is determined by the Gibbs-Helmholtz equation with the thermodynamic parameters ΔH° , T° , and ΔC_p and connected to the measured signal ($[\theta]_{222nm}$) via the baseline parameters θ_{F0} , θ_{U0} , m_F , and m_U as described in detail in *Chapter II*. These parameters are used to fit the data and stand for the temperature where $\Delta G = 0$ (T°), the enthalpy at T° (ΔH°), the change of heat capacity upon unfolding (ΔC_p), the ellipticities of the fully folded and fully unfolded state at 0 °C (θ_{F0} and θ_{U0}), and the temperature slopes of the ellipticities of the fully folded and fully unfolded state (m_F and m_U). The data was fitted by different models from $n = 2 \dots 6$, with $v_1 = v_2$ for even n and $v_1 = v_2 + 1$ for odd n in the case of hetero coiled coils and $v_1 = n$ in the case of homo coiled coils of E and K. The fitting procedure is explained in *Chapter II* also. The different models were compared on the basis of the root mean square errors (RMSE) of the fits.

VESICLE FUSION EXPERIMENTS

In all fusion experiments CPE containing vesicles were mixed in a 1 : 1 ratio with vesicles containing CPK, $CPK_2O_2K_2$ or CPO_3K_3 , total lipid concentrations were 0.1 mM and lipopeptides in the bilayers were at 1 mol%. Size increase was measured using a Malvern Zetasizer nano-s. Before mixing, vesicle solutions showed only one population with a hydrodynamic radius (r_h) of ~50 nm. After mixing, the size was measured every 2 minutes for 60 minutes and generally two populations were

observed: one at a relatively constant radius of 40 - 80 nm which had decreasing intensity and another with increasing r_h and increasing intensity. The latter population was interpreted as the size increase.

For lipid mixing, CPE containing vesicles contained additionally 0.5 mol% LR-DOPE and 0.5 mol% NBD-DOPE. After mixing in a black 96 well plate, NBD-DOPE fluorescence emission was measured using a Tecan infinite M1000 pro plate reader. Excitation and emission wavelengths were 460 nm and 535 nm respectively and both bandwidths were 10 nm. The fluorescence increase ΔF was calculated by:

$$\Delta F = \frac{F - F_0}{F_{max} - F_0}, \quad (5)$$

with the fluorescence emission F , and the reference values F_{max} and F_0 . In lipid mixing experiments F_0 was the fluorescence emission of CPE labeled vesicles mixed with vesicles containing no lipopeptides and F_{max} was the fluorescence emission of vesicles containing only half the dyes NBD-DOPE and LR-DOPE.

For content mixing experiments CPE labeled liposomes (total lipid concentration 1 mM) were formed in a 20 mM solution of sulforhodamine B in TES buffer. The vesicles were separated from excess dye by means of a sephadex G-50 column. The vesicle containing fraction was collected and diluted to a total volume of 10 ml to reach a final total lipid concentration of ~ 0.1 mM. After vesicle mixing, sulforhodamine B emission was monitored at 580 nm using an excitation wavelength of 520 nm and bandwidths of 10 nm. The fluorescence increase was calculated using equation (5), with F_0 being the fluorescence intensity of sulphorhodamine B loaded CPE vesicles mixed with empty vesicles and F_{max} being the fluorescence intensity of sulforhodamine B loaded CPE vesicles lysed with 10 vol% Triton X-100.

REFERENCES

- (1) Robson Marsden, H.; Korobko, A. V.; Zheng, T.; Voskuhl, J.; Kros, A., Controlled liposome fusion mediated by SNARE protein mimics. *Biomaterials Science* **2013**, *1*, 1046.
- (2) Robson Marsden, H.; Elbers, Nina A.; Bomans, Paul H. H.; Sommerdijk, Nico A. J. M.; Kros, A., A Reduced SNARE Model for Membrane Fusion. *Angew. Chem. Int. Ed.* **2009**, *48*, 2330.
- (3) Tomatsu, I.; Marsden, H. R.; Rabe, M.; Versluis, F.; Zheng, T.; Zope, H.; Kros, A., Influence of pegylation on peptide-mediated liposome fusion. *J. Mater. Chem.* **2011**, *21*, 18927.
- (4) Versluis, F.; Dominguez, J.; Voskuhl, J.; Kros, A., Coiled-coil driven membrane fusion: zipper-like vs. non-zipper-like peptide orientation. *Faraday Discuss.* **2013**, *166*, 349.
- (5) Versluis, F.; Voskuhl, J.; van Kolck, B.; Zope, H.; Bremmer, M.; Albregtse, T.; Kros, A., In Situ Modification of Plain Liposomes with Lipidated Coiled Coil Forming Peptides Induces Membrane Fusion. *J. Am. Chem. Soc.* **2013**, *135*, 8057.
- (6) Zheng, T. T.; Voskuhl, J.; Versluis, F.; Zope, H. R.; Tomatsu, I.; Marsden, H. R.; Kros, A., Controlling the rate of coiled coil driven membrane fusion. *Chem. Commun.* **2013**, *49*, 3649.
- (7) Rothman, J. E., The Principle of Membrane Fusion in the Cell (Nobel Lecture). *Angew. Chem. Int. Ed.* **2014**.
- (8) Südhof, T. C.; Rothman, J. E., Membrane fusion: grappling with SNARE and SM proteins. *Science* **2009**, *323*, 474.
- (9) Jahn, R.; Fasshauer, D., Molecular machines governing exocytosis of synaptic vesicles. *Nature* **2012**, *490*, 201.
- (10) Hui, E.; Johnson, C. P.; Yao, J.; Dunning, F. M.; Chapman, E. R., Synaptotagmin-Mediated Bending of the Target Membrane Is a Critical Step in Ca²⁺-Regulated Fusion. *Cell* **2009**, *138*, 709.
- (11) Kozlov, M. M.; McMahan, H. T.; Chernomordik, L. V., Protein-driven membrane stresses in fusion and fission. *Trends Biochem. Sci.* **2010**, *35*, 699.
- (12) McMahan, H. T.; Kozlov, M. M.; Martens, S., Membrane Curvature in Synaptic Vesicle Fusion and Beyond. *Cell* **2010**, *140*, 601.
- (13) Campelo, F.; McMahan, H. T.; Kozlov, M. M., The hydrophobic insertion mechanism of membrane curvature generation by proteins. *Biophys. J.* **2008**, *95*, 2325.
- (14) Martelli, G.; manuscript in preparation
- (15) Woolfson, D. N. In *Adv. Protein Chem.*; David, A. D. P., John, M. S., Eds.; Academic Press: 2005; Vol. Volume 70, p 79.
- (16) Grigoryan, G.; Keating, A. E., Structural specificity in coiled-coil interactions. *Curr. Opin. Struct. Biol.* **2008**, *18*, 477.
- (17) Gautier, R.; Douguet, D.; Antonny, B.; Drin, G., HELIQUEST: a web server to screen sequences with specific α -helical properties. *Bioinformatics* **2008**, *24*, 2101.
- (18) Segrest, J. P.; De Loof, H.; Dohlman, J. G.; Brouillette, C. G.; Anantharamaiah, G. M., Amphipathic helix motif: Classes and properties. *Proteins: Structure, Function, and Bioinformatics* **1990**, *8*, 103.
- (19) Segrest, J. P.; Jones, M. K.; Mishra, V. K.; Anantharamaiah, G. M. In *Curr. Top. Membr.*; Sidney A. Simon, T. J. M., Ed.; Academic Press: 2002; Vol. Volume 52, p 397.
- (20) Hristova, K.; Wimley, W. C.; Mishra, V. K.; Anantharamiah, G. M.; Segrest, J. P.; White, S. H., An amphipathic α -helix at a membrane interface: a structural study using a novel X-ray diffraction method. *J. Mol. Biol.* **1999**, *290*, 99.
- (21) Mishra, V. K.; Palgunachari, M. N.; Segrest, J. P.; Anantharamaiah, G. M., Interactions of synthetic peptide analogs of the class A amphipathic helix with lipids. Evidence for the snorkel hypothesis. *J. Biol. Chem.* **1994**, *269*, 7185.
- (22) Segrest, J. P.; Deloof, H.; Dohlman, J. G.; Brouillette, C. G.; Anantharamaiah, G. M., Amphipathic Helix Motif - Classes and Properties. *Proteins* **1990**, *8*, 103.
- (23) Segrest, J. P.; Jones, M. K.; De Loof, H.; Brouillette, C. G.; Venkatachalapathi, Y. V.; Anantharamaiah, G. M., The amphipathic helix in the exchangeable apolipoproteins: a review of secondary structure and function. *J. Lipid Res.* **1992**, *33*, 141.
- (24) Mishra, V. K.; Palgunachari, M. N., Interaction of Model Class A1, Class A2, and Class Y Amphipathic Helical Peptides with Membranes. *Biochemistry* **1996**, *35*, 11210.

- (25) Palgunachari, M. N.; Mishra, V. K.; Lund Katz, S.; Phillips, M. C.; Adeyeye, S. O.; Alluri, S.; Anantharamaiah, G. M.; Segrest, J. P., Only the two end helices of eight tandem amphipathic helical domains of human apo A-I have significant lipid affinity. Implications for HDL assembly. *Arteriosclerosis, thrombosis, and vascular biology* **1996**, *16*, 328.
- (26) Vu, C.; Robblee, J.; Werner, K. M.; Fairman, R., Effects of charged amino acids at b and c heptad positions on specificity and stability of four-chain coiled coils. *Protein Sci.* **2001**, *10*, 631.
- (27) Ryan, S. J.; Kennan, A. J., Variable Stability Heterodimeric Coiled-Coils from Manipulation of Electrostatic Interface Residue Chain Length. *J. Am. Chem. Soc.* **2007**, *129*, 10255.
- (28) Pendley, S. S.; Yu, Y. B.; Cheatham, T. E., Molecular dynamics guided study of salt bridge length dependence in both fluorinated and non-fluorinated parallel dimeric coiled-coils. *Proteins-Structure Function and Bioinformatics* **2009**, *74*, 612.
- (29) Mason, J. M.; Arndt, K. M., Coiled coil domains: stability, specificity, and biological implications. *Chembiochem* **2004**, *5*, 170.
- (30) Chen, Y.-H.; Yang, J. T.; Chau, K. H., Determination of the helix and β form of proteins in aqueous solution by circular dichroism. *Biochemistry* **1974**, *13*, 3350.
- (31) Gans, P. J.; Lyu, P. C.; Manning, M. C.; Woody, R. W.; Kallenbach, N. R., The helix-coil transition in heterogeneous peptides with specific side-chain interactions: Theory and comparison with CD spectral data. *Biopolymers* **1991**, *31*, 1605.
- (32) Greenfield, N. J., Using circular dichroism collected as a function of temperature to determine the thermodynamics of protein unfolding and binding interactions. *Nat Protoc* **2006**, *1*, 2527.
- (33) Marky, L. A.; Breslauer, K. J., Calculating thermodynamic data for transitions of any molecularity from equilibrium melting curves. *Biopolymers* **1987**, *26*, 1601.
- (34) Job, P., Recherches sur la formation de complexes minéraux en solution, et sur le stabilite. *Ann. Chim.-Paris* **1928**, *9*, 113.
- (35) Gil, V. M. S.; Oliveira, N. C., On the use of the method of continuous variations. *J. Chem. Educ.* **1990**, *67*, 473.
- (36) Litowski, J. R.; Hodges, R. S., Designing heterodimeric two-stranded alpha-helical coiled-coils. Effects of hydrophobicity and alpha-helical propensity on protein folding, stability, and specificity. *J. Biol. Chem.* **2002**, *277*, 37272.
- (37) Olson, E. J.; Bühlmann, P., Getting More out of a Job Plot: Determination of Reactant to Product Stoichiometry in Cases of Displacement Reactions and n:n Complex Formation. *The Journal of Organic Chemistry* **2011**, *76*, 8406.
- (38) Breslauer, K. J. In *Methods Enzymol.*; Michael L. Johnson, G. K. A., Ed.; Academic Press: 1995; Vol. Volume 259, p 221.
- (39) Doyle, C. M.; Rumfeldt, J. A.; Broom, H. R.; Broom, A.; Stathopoulos, P. B.; Vassall, K. A.; Almey, J. J.; Meiering, E. M., Energetics of oligomeric protein folding and association. *Arch. Biochem. Biophys.* **2013**, *531*, 44.
- (40) Marsden, H. R.; Tomatsu, I.; Kros, A., Model systems for membrane fusion. *Chem. Soc. Rev.* **2011**, *40*, 1572.
- (41) Struck, D. K.; Hoekstra, D.; Pagano, R. E., Use of resonance energy transfer to monitor membrane fusion. *Biochemistry* **1981**, *20*, 4093.

APPENDIX

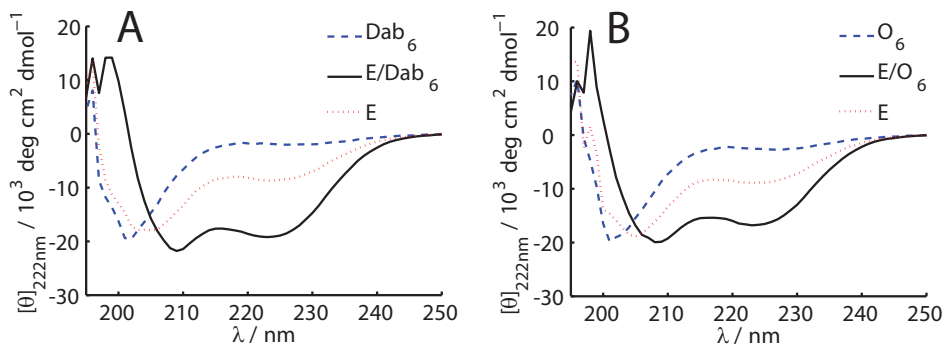


Figure A1. CD spectra of (A) Dab₆, E/Dab₆ [E] : [Dab₆] = 2 : 1, and E (B) O₆, E/O₆ [E] : [O₆] = 1 : 1, and E at total peptide concentrations of 200 μM in PBS.

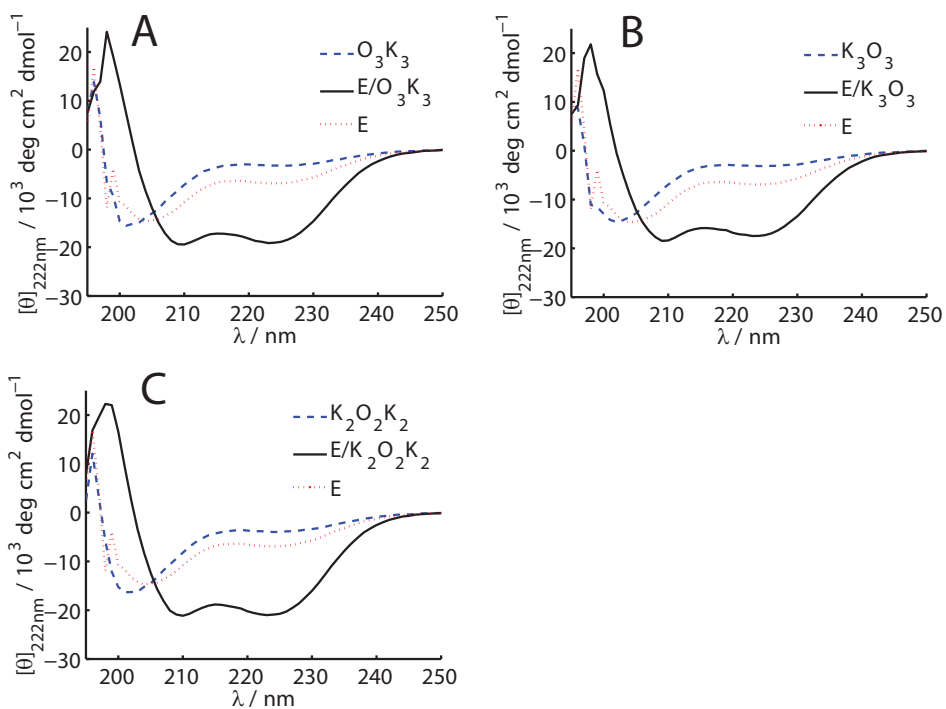


Figure A2. CD spectra of (A) O₃K₃, E/O₃K₃ [E] : [O₃K₃] = 1 : 1, and E (B) K₃O₃, E/K₃O₃ [E] : [K₃O₃] = 1 : 1, and E (C) K₂O₂K₂, E/K₂O₂K₂ [E] : [K₂O₂K₂] = 1 : 1, and E at total peptide concentrations of 200 μM in PBS.

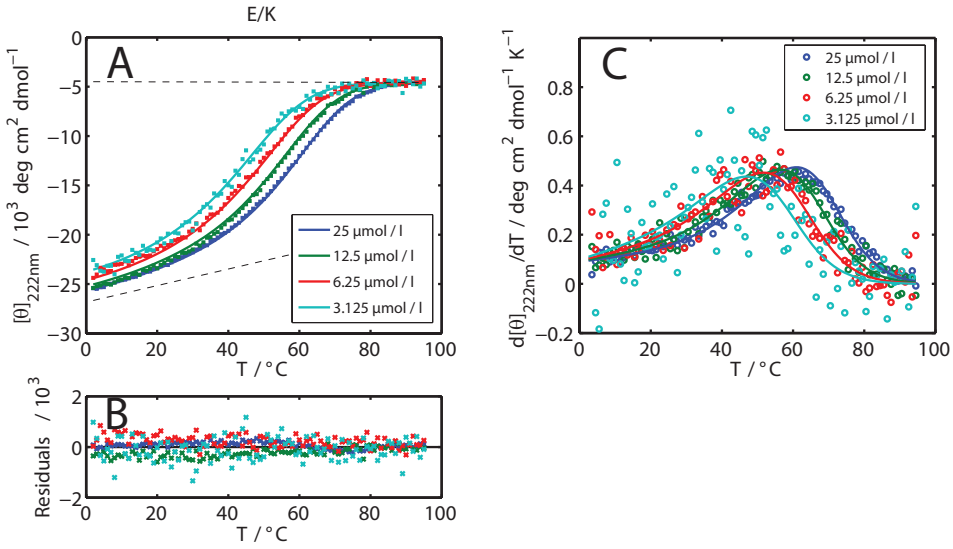


Figure A3. (A) Thermal denaturation data (squares) and best fitting model ($v_1 = v_2 = 1$; solid lines) with baselines (broken lines) of E/K. (B) Residuals of best fit. (C) First derivative of data (circles) and best fitting model (solid lines). Concentration of the coiled coil complex given in the key.

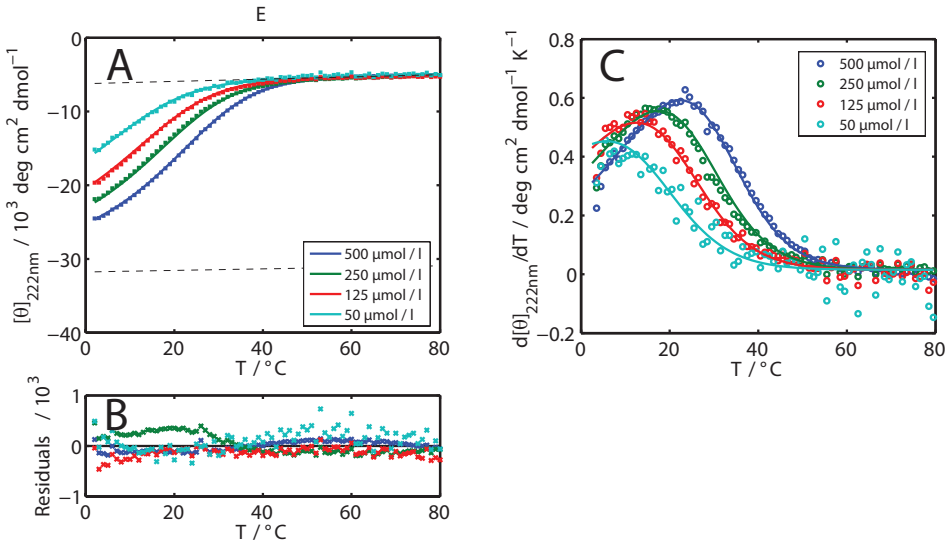


Figure A4. (A) Thermal denaturation data (squares) and best fitting model ($v_1 = n = 2$; solid lines) with baselines (broken lines) of E. (B) Residuals of best fit. (C) First derivative of data (circles) and best fitting model (solid lines). Concentration of the coiled coil complex given in the key.

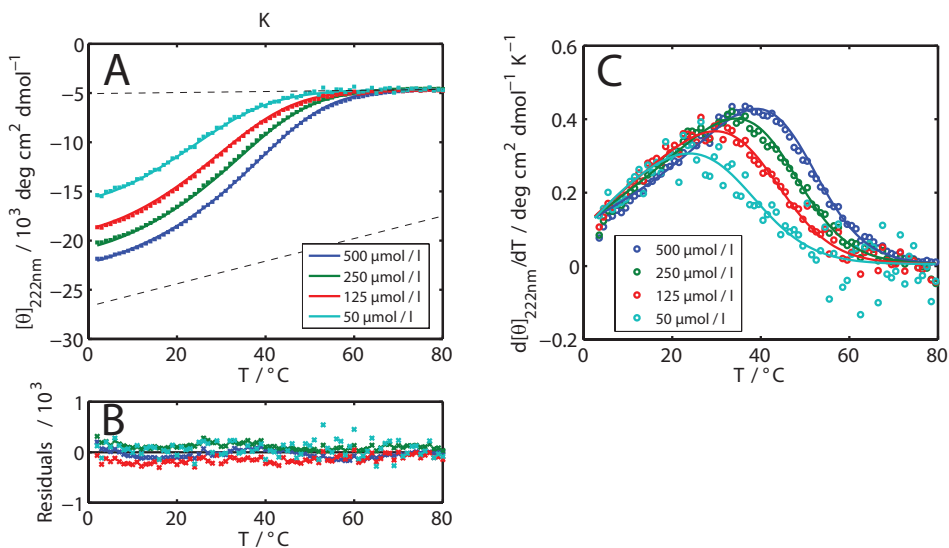


Figure A5. (A) Thermal denaturation data (squares) and best fitting model ($v_1 = n = 2$; solid lines) with baselines (broken lines) of K. (B) Residuals of best fit. (C) First derivative of data (circles) and best fitting model (solid lines). Concentration of the coiled coil complex given in the key.

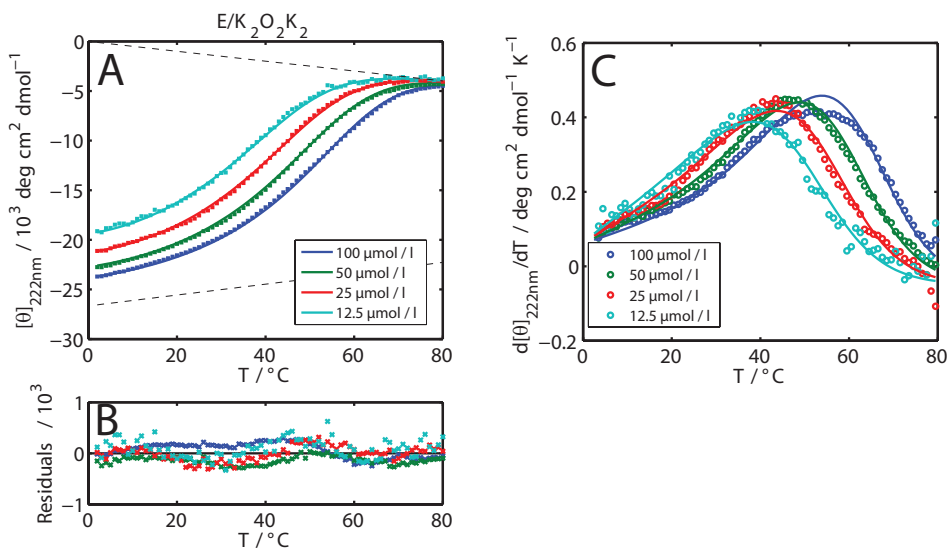


Figure A6. (A) Thermal denaturation data (squares) and best fitting model ($v_1 = n = 2$; solid lines) with baselines (broken lines) of E/K₂O₂K₂. (B) Residuals of best fit. (C) First derivative of data (circles) and best fitting model (solid lines). Concentration of the coiled coil complex given in the key.

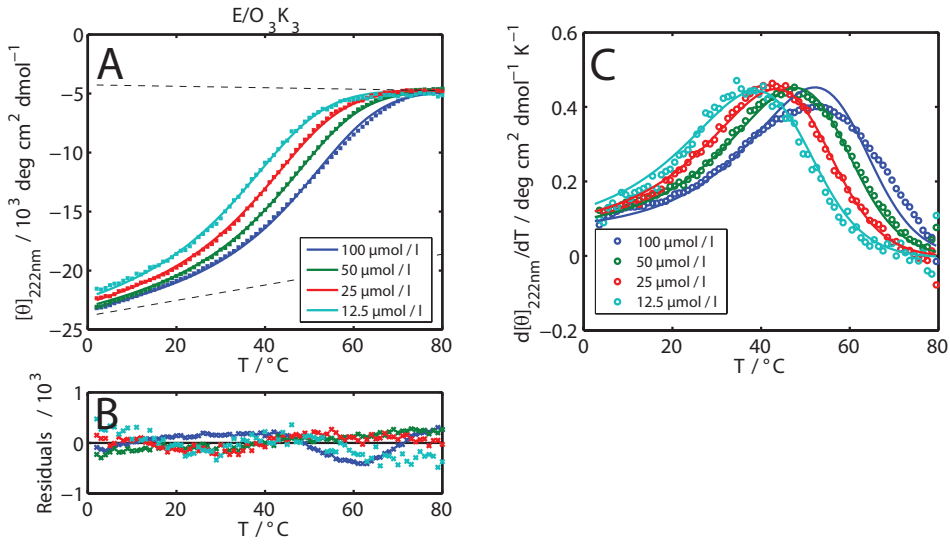


Figure A7. (A) Thermal denaturation data (squares) and best fitting model ($v_1 = v_2 = 1$; solid lines) with baselines (broken lines) of E/O₃K₃, (B) Residuals of best fit. (C) First derivative of data (circles) and best fitting model (solid lines). Concentration of the coiled coil complex given in the key.

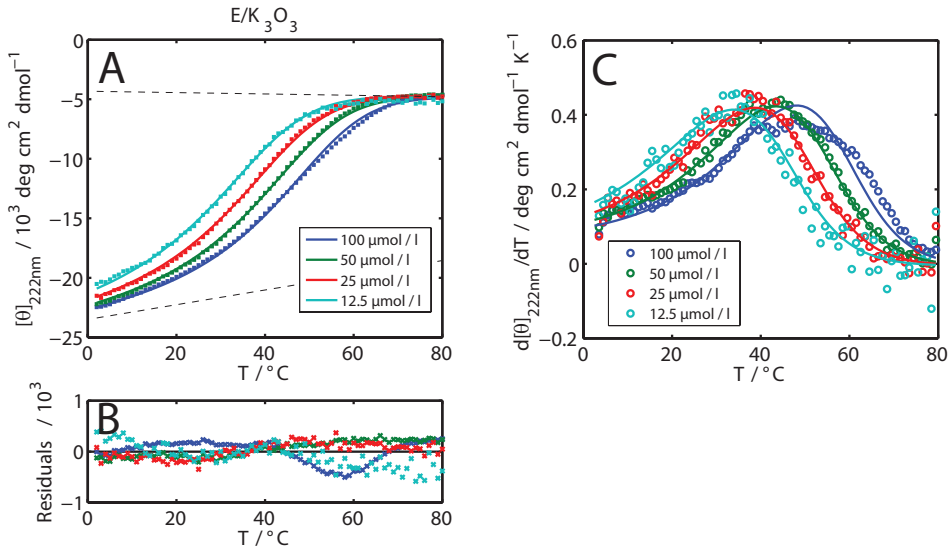


Figure A8. (A) Thermal denaturation data (squares) and best fitting model ($v_1 = v_2 = 1$; solid lines) with baselines (broken lines) of E/K₃O₃, (B) Residuals of best fit. (C) First derivative of data (circles) and best fitting model (solid lines). Concentration of the coiled coil complex given in the key.

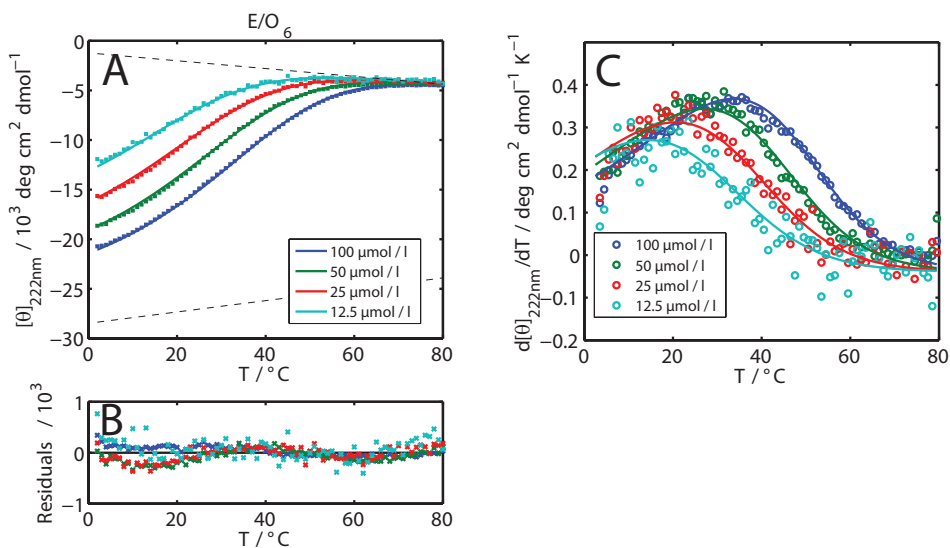


Figure A9. (A) Thermal denaturation data (squares) and best fitting model ($v_1 = v_2 = 1$; solid lines) with baselines (broken lines) of E/O₆. (B) Residuals of best fit. (C) First derivative of data (circles) and best fitting model (solid lines). Concentration of the coiled coil complex given in the key.

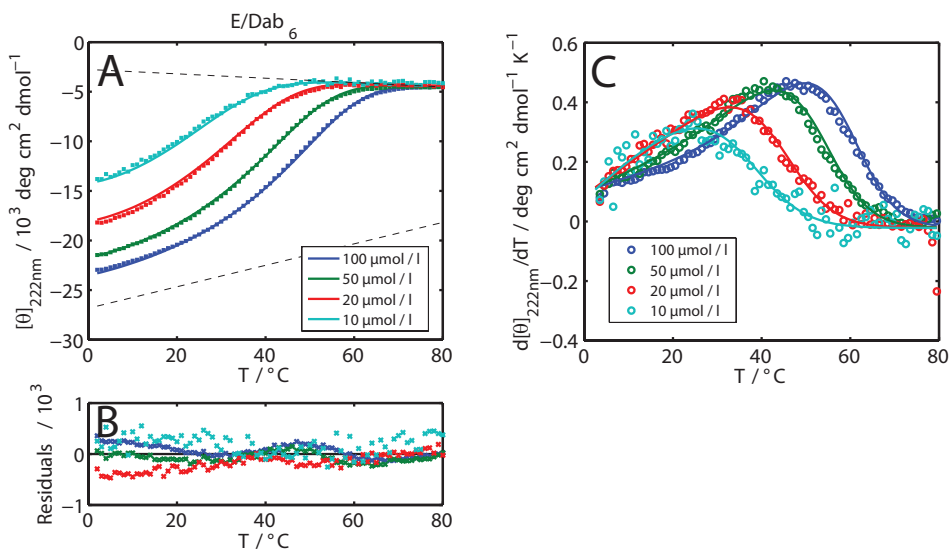


Figure A10. (A) Thermal denaturation data (squares) and best fitting model ($v_1 = 2, v_2 = 1$; solid lines) with baselines (broken lines) of E/Dab₆. (B) Residuals of best fit. (C) First derivative of data (circles) and best fitting model (solid lines). Concentration of the coiled coil complex given in the key.

Table A1. Thermodynamic and baseline parameters of best fitting models for the thermal unfolding of coiled coil complexes.

	Model	ΔH° (kJ mol ⁻¹)	T° (°C)	ΔC_P (kJ mol ⁻¹ K ⁻¹)	θ_{F0} (10 ³ deg cm ² d mol ⁻¹)	m_F (deg cm ² d mol ⁻¹ K ⁻¹)	θ_{U0} (10 ³ deg cm ² d mol ⁻¹)	m_U (deg cm ² d mol ⁻¹ K ⁻¹)
E/K	A ₁ B ₁	263.3	120.8	-2.1	-26.838	83.9	-4.491	-0.9
E/KDab	A ₂ B ₁	386.4	116.9	-3.3	-26.617	103.4	-3.582	-12.4
E/O3K3	A ₁ B ₁	221.5	107.1	-1.5	-23.811	64.9	-4.263	-6.1
E/K3O3	A ₁ B ₁	208.5	106.4	-1.4	-23.480	61.7	-4.320	-5.7
E/K2O2K2	A ₁ B ₁	230.6	111.6	-2.0	-26.684	56.1	0	-49.9
E/Korn	A ₁ B ₁	168.4	112.9	-1.2	-28.534	65.9	-1.183	-39.9
K/K	A ₂	198.4	77.3	-2.5	-26.764	119.3	-5.036	5.1
E/E	A ₂	163.2	61.5	-1.7	-32.022	34.2	-6.202	14.9

